International Journal of Heat and Technology
Vol. 44, No. 2, April, 2026, pp. 551-560
Journal homepage: http://iieta.org/journals/ijht

Experimental Investigation of an Innovative Coaxial with Shell-and-Tube Heat Exchanger: Thermo-Hydraulic Performance Evaluation and Comparative Analysis

Chabane Medjdoub[1*], Abdelhakim Benslimane[2], Djamel Sadaoui[2]

[1] Centre de Recherche en Technologies Agro-Alimentaires, Route de Targa Ouzemmour, Campus Universitaire, Bejaia 06000, Algeria
[2] Laboratoire de Mécanique, Matériaux et Energétique (L2ME), Faculté de Technologie, Université de Bejaia, Bejaia 06000, Algeria

Corresponding Author Email: chabane.medjdoub@crtaa.dz

https://doi.org/10.18280/ijht.440210

Received: 31 January 2026
Revised: 2 April 2026
Accepted: 11 April 2026
Available online: 30 April 2026

Keywords:
coaxial with shell-and-tube heat exchanger, shell-and-tube heat exchanger, thermo-hydraulic performance, heat transfer enhancement, pressure drop, Number of Transfer Units method

ABSTRACT

An innovative heat exchanger configuration, referred to as the coaxial with shell-and-tube heat exchanger (CWST), was experimentally investigated and compared with a conventional shell-and-tube heat exchanger (STHE) in terms of thermo-hydraulic performance. A test bench was developed to evaluate both heat exchangers under identical operating conditions. Temperature, pressure, and flow rate data were collected at the inlet and outlet sections using calibrated sensors. The thermal and hydraulic performances were analysed based on heat transfer rate, heat flux, and pressure drop characteristics. The experimental results demonstrated that the proposed CWST achieved enhanced heat transfer performance with a lower pressure drop compared with the conventional STHE, resulting in a superior heat-transfer-to-pressure-drop ratio. In addition, the experimental results were compared with theoretical predictions obtained using the Number of Transfer Units (NTU) method for the STHE, and consistent trends were observed. The improved performance of the CWST was attributed to its modified flow configuration, which promoted more effective thermal interaction between the working fluids. The proposed geometry, therefore, shows strong potential for application in compact and energy-efficient thermal systems.

1. INTRODUCTION

Heat exchangers are categorized into various types according to their structural configurations, including helical coil and plate-frame heat exchangers. However, the widely favored choice in industrial applications remains the shell-and-tube heat exchanger (STHE). Renowned for its large surface area, compact design, and efficient heat transfer, the STHE finds extensive use in sectors reliant on heat transfer to facilitate chemical processes. Such processes include distillation, synthesis, and combustion, commonly observed in petrochemical, food, and pharmaceutical industries. Additionally, STHE plays a crucial role in converting atomic and fossil energy into electricity, as seen in power stations. Their applications also extend to air-conditioning, heating, and heat pump systems [1], where they contribute to temperature control and thermal regulation in enclosed environments such as cold storage facilities.

The necessity to enhance heat exchanger thermo-hydraulic performances arises from the depletion of energy resources, environmental challenges linked to pollution-induced climate change, and the global pursuit of economic prosperity by nations. A substantial body of literature is dedicated to heat exchanger studies, encompassing both numerical and experimental perspectives. The predominant goal across these works is the enhancement of heat transfer [2] and the reduction of pressure drop within these devices. Several representative studies and enhancement approaches related to heat exchanger thermo-hydraulic performance are briefly reviewed below.

The thermo-hydraulic performance of heat exchangers is strongly influenced by the characteristics of the heat transfer tubes. Several studies have delved into the impact of tube shapes, including those that are finned, twisted or coiled. Tan et al. [3] employed simulation to investigate heat exchangers featuring twisted oval tubes and finned tubes. They found that these non-circular shapes enhanced turbulence, particularly in comparison to smooth circular tubes. The utilization of finned tubes, in particular, was observed to improve the transfer surface area, consequently boosting the heat exchange rate. In the case of twisted oval tube heat exchangers, the length of the torsion pitch was identified as a significant factor affecting transfer performance. Zhang et al. [4] investigated the thermal-hydraulic characteristics of twisted tubes in turbulent flow and reported that a reduction in twist pitch yields higher heat transfer rates, though this is accompanied by a proportional increase in the friction factor. Dizaji et al. [5] conducted experiments on a vertical heat exchanger employing coil tubes and injecting air bubbles. Their findings demonstrated that this process elevated efficiency and the Number of Transfer Units (NTU) of the examined exchanger. Additionally, Genić et al.

[6] experimentally investigated the thermo-hydraulic performance of a spiral-coil heat exchanger and demonstrated that heat transfer enhancement could be achieved by increasing the coil diameter, pitch length, and flow rate.

Other research has examined the characteristics of baffles and how they affect the thermos-hydraulic performances of heat exchangers. An experimental investigation comparing segmented and overlapping helical baffles in STHEs was carried out by Zhang et al. [7] by employing oil as the fluid flow. According to their research, the latter kind of exchanger outperformed the former in terms of heat transfer per unit pressure drop at the same flow rate and showed a smaller pressure drop throughout the shell. When Xiao et al. [8] simulated an STHE using helical baffles at different inclination degrees and Prandtl values, they discovered that water had superior heat transfer at a 40° baffle angle, whereas fluids with large Prandtl values showed improved heat transfer at lower inclination angles. The study highlighted that helical baffle exchangers incurred lower pressure drop compared to those featuring segmented baffles. Li et al. [9] used a tube bundle of 19 tubes in a single pass and creative baffle designs to do computational and experimental studies on an STHE. A 2.32 million cell mesh grid was used with a realizable k-ε model in their investigation. Ben Slimene et al. [10] employed simulation to explore turbulent flows in an STHE with different passes, introducing baffles to enhance thermos-hydraulic performances. They used the Shear Stress Transport (SST) k-ω turbulence model and extended it to an STHE configuration with a rectangular shell. Ali et al. [11] provided a concise summary of significant types of heat exchangers and passive techniques for improving heat transfer by focusing on the use of baffles [12].

Additional research has explored various types of baffles, including rod baffles. The STHEs with rod baffles, three-flow baffles, and pore plate baffles were the subjects of comparative research by Chen et al. [13]. In conclusion, the segmented baffle heat exchanger was found to have inferior thermo-hydraulic performance to all of these configurations. Wang et al. [14] examined an STHE with two shell passes and rod baffles in experimental research. And according to the results, it performed better than a single shell pass exchanger with the same kind of baffles. Liu et al. [15] performed a comparative simulation of two rod-baffle STHEs, evaluating the thermo-hydraulic performances of plain tubes against spirally corrugated tubes. The results demonstrated that the corrugated tube configuration achieved superior thermo-hydraulic performances.

Fascinating and innovative research endeavors have yielded novel designs and structures. In a study by Ji et al. [16], a simulation was conducted on an STHE featuring elastic tubes. The findings revealed that an increasing heat transfer was achieved by adding vibrations to the shell side, particularly for low Reynolds number flows. Bougriou and Baadache [17] introduced a novel heat exchanger termed a dual concentric tube and shell heat exchanger. This design not only amplifies the exchange surface but also augments heat transfer within a more compact volume. Van Trang et al. [18] conducted an experiment to evaluate the thermo-hydraulic performances of a four-pass micro-scooter radiator that uses ambient air to cool hot water. The study unveiled that, under certain water flow rates, the cooling efficiency improved with the use of a fan, surpassing that of conventional radiators with larger dimensions. Additionally, it was observed that while fuel consumption decreased, engine power increased, leading to a reduction in the mini radiator operating cost compared to larger conventional counterparts.

Considerable attention has been devoted to plate heat exchangers and the application of nanofluids for heat transfer enhancement. Lozano et al. [19] conducted numerical and experimental investigations on a grooved plate heat exchanger using oil and water as working fluids in automotive applications. The study revealed non-uniform fluid flows and indicated a tendency for the two fluids to move along the plates' lateral extremities. Elias et al. [20], Leong et al. [21], and Elias et al. [22] investigated the effects of nanofluids on STHE. The first group investigated baffles with different inclination angles and reported that nanofluids enhanced thermo-hydraulic performance. The second group compared nanofluids with ethylene glycol and water, determining that nanofluids resulted in superior overall heat transfer and convection coefficients. The third group concluded that the shape, volume concentration, and particle size of the constituents in nanofluids significantly influenced heat exchanger thermo-hydraulic performance. Philip et al. [23] carried out experiments on the properties of magnetic nanoparticles and observed an increase in thermal conductivity when controlled by an external magnetic field. Yu et al. [24] further explored graphene nanosheets dispersed in ethylene glycol and reported an increase in thermal conductivity owing to their favourable thermophysical properties.

An alternative method for studying heat exchangers is to use optimization methods of non-linear calculation algorithms. Touatit and Bougriou [25] conducted an optimization study on a triple concentric tube heat exchanger in which nitrogen, oxygen, and hydrogen were circulated through three separate channels. They used a Fortran-based computation code and a techno-economic method to calculate heat transfer coefficients, total friction power, and temperature profiles. Ultimately, they identified optimum diameters that minimized energy consumption and manufacturing costs. Xie et al. [26], Fettaka et al. [27], and Guo et al. [28] optimized the STHE thermo-hydraulic performance using non-linear prediction systems. The first group employed the artificial neural method, the second utilized the multi-objective optimization method, and the third employed the genetic algorithm. Optimization research on an STHE was carried out by Şahin et al. [29] utilizing the artificial bee colony approach. Upon comparing their results with existing literature, they concluded that this method effectively minimizes manufacturing and operating costs. In another study, Guo et al. [30] optimized an STHE by maximizing the objective function describing the synergy field number. This number signifies the synergy between heat transfer and the velocity field, leading to the conclusion that its use yields superior thermo-hydraulic performances and design cost compared to the traditional method for reducing the objective function that characterizes the overall cost. To minimize total expenditures, Fesanghary et al. [31] explored STHE optimization using the harmony search method combined with global sensitivity analysis. Their findings indicate that this integrated approach yields significantly more precise results compared to traditional genetic algorithms.

This study presents an experimental investigation of a coaxial with shell-and-tube heat exchanger (CWST), comparing its thermo-hydraulic performances to a conventional STHE design. The results demonstrate that the CWST achieves higher heat flux and lower pressure drop. While heat transfer rates are comparable between the two models, the CWST exhibits a superior heat transfer rate to

pressure drop ratio. Furthermore, these experimental findings are consistent with the numerical simulations reported by Medjdoub et al. [32] regarding both thermal and hydraulic performances.

2. EXPERIMENTAL SETUP

To compare the thermo-hydraulic performances of the STHE with those of the CWST heat exchanger, a test bench was developed to accommodate both heat exchangers and evaluate both units experimentally. This test bench has two water tanks for cold water and two water tanks for hot water (the two main water tanks for hot and cold water are insulated from the outside, as shown in Figure 1). These water tanks ensure temperature homogeneity by circulating water from the main tank to the secondary one, and thus preventing the direct return of exchanger outlet water to the main tank.

This test bench also has tubes (those connected to the heat exchanger inlets are insulated from the outside using wadding), and has temperature, pressure, and flow sensors that enable us to measure the thermo-hydraulic performances of the two heat exchangers.

The sensors are analog and have a manufacturer-specified accuracy of ±0.5 °C for temperature, ±1 psi for pressure, and ±0.1 l/min for volume flow rate. To ensure data reliability, each measurement point was recorded manually only after reaching a stable steady state. Each experimental run was performed in duplicate to verify the reproducibility of the results; the deviations between successive tests were found to be within the sensors' uncertainty range, confirming the consistency of the data.

The experiments were conducted under laboratory conditions at a constant ambient temperature of 18 °C throughout the entire experiment, with no wind or external interference. This helps to ensure the reliability of the results.

A system of several valves is used to perform the following tasks, by choosing whether to open or close the appropriate ones:

- Mixing hot and cold water from the main tanks in a closed circuit to homogenize temperature.
- Sending the water from the main tanks to the heat exchanger, then to the secondary tanks.
- Sending water from secondary tanks to main tanks.
- Adjustment of the fluid flow rate (by adjusting the opening angle of the valve).

Figure 1. Test bench used for the experimental study

Figures 2-4 show the STHE used in the comparative study of this article, and Figure 5 illustrates the copper tube bundle, with its geometrical dimensions summarized in Table 1. The tube sheets are made of copper and welded to the tubes, then a thickness of metallic glue is added to reinforce the structure, and a thickness of silicone is added to mainly reduce heat transfer through the tube sheets and focus on heat transfer through the tubes, as reported by Medjdoub et al. [32]. The tube bundle is built using the 30° triangular configuration, and a maximum number of tubes is employed to maximize heat transfer. The STHE is installed on the test bench at the position designated for the CWST heat exchanger, as illustrated in Figure 6. In this configuration, valves 6 and 11 are closed, as the unit features only two inlet and two outlet nozzles.

Figure 2. Shell-and-tube heat exchanger (STHE) without distributors

Figure 3. Shell-and-tube heat exchanger (STHE) with distributors

Figure 4. Shell-and-tube heat exchanger (STHE) insulated with polystyrene

Figure 5. Tube bundle of the shell-and-tube heat exchanger (STHE)

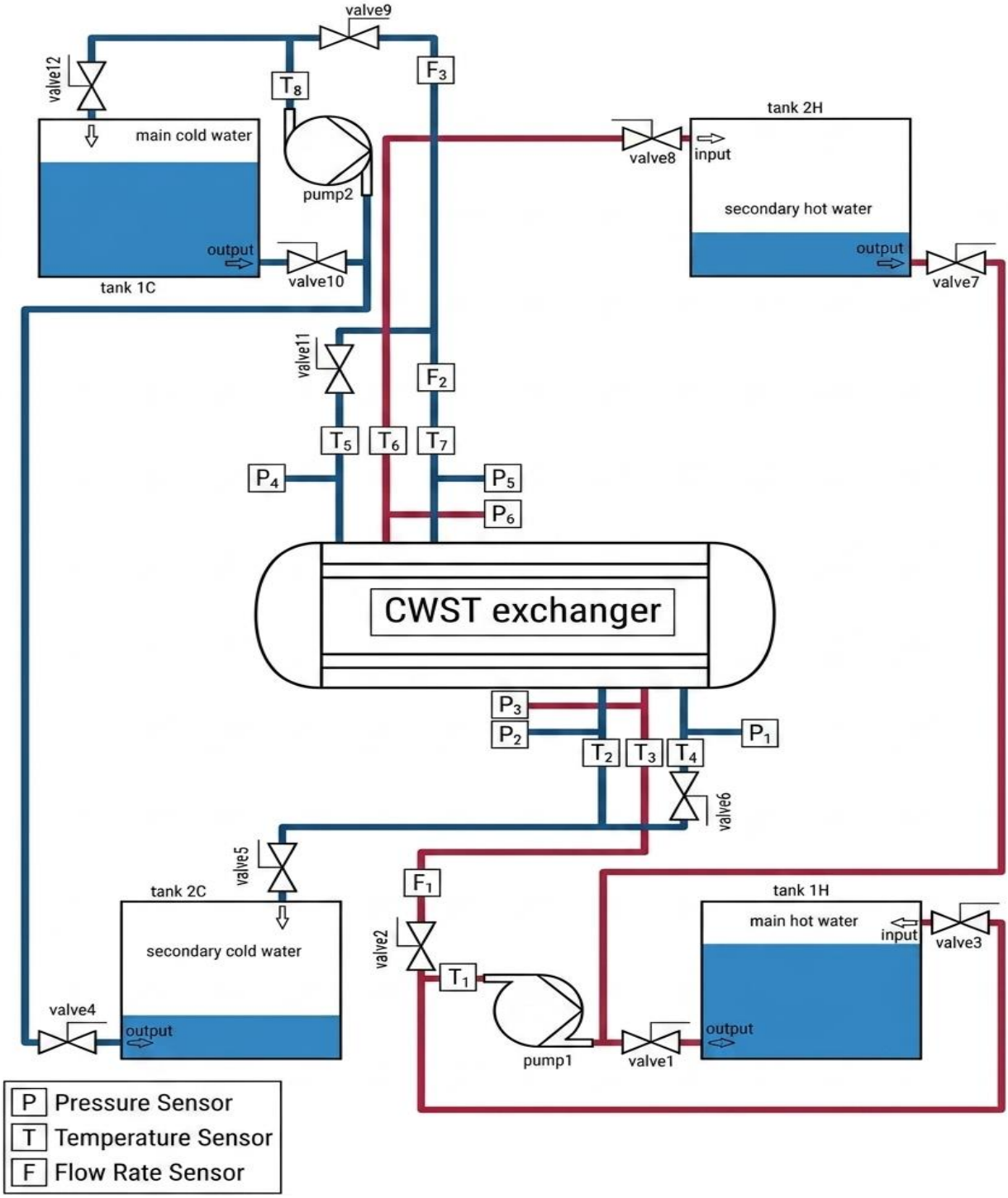

Figure 6. The test bench's technical diagram

Table 1. Geometrical dimensions of the shell-and-tube heat exchanger (STHE)

Geometrical Dimension	Value
Shell inner diameter, Ds [m]	0.13
Shell length, L [m]	0.6
Number of tubes, Nt	37
Pitch, Pt [m]	0.018
Tube external diameter, do [m]	0.014
$PR = \frac{Pt}{do}$	1.285
Tube thickness, e [m]	0.001
Tube inner diameter, di [m]	0.012

Figure 7. Coaxial with shell-and-tube heat exchanger (CWST) without the last distributors, their tube sheets, and the tubes connected to them

Figure 8. Coaxial with shell-and-tube heat exchanger (CWST) without last distributors

Figure 9. Coaxial with shell-and-tube heat exchanger (CWST) with all its distributors

Figure 10. Coaxial with shell-and-tube heat exchanger (CWST) insulated with polystyrene

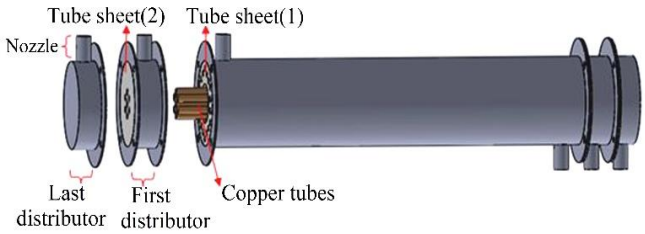

Figure 11. The coaxial with shell-and-tube heat exchanger's (CWST) internal geometry

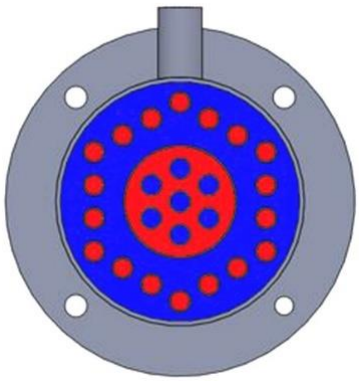

Figure 12. The coaxial with shell-and-tube heat exchanger's (CWST) transverse section showing the hot (in red) and cold (in blue) fluids

Figure 13. The coaxial with shell-and-tube heat exchanger's (CWST) longitudinal section showing the hot (in red) and cold (in blue) fluids

Table 2. Coaxial with shell-and-tube exchanger (CWST) compared with shell-and-tube heat exchanger (STHE)

Design Parameters	Coaxial With Shell-and-Tube Heat Exchanger (CWST)	Shell-and-Tube Heat Exchanger (STHE)
Tube bundle	25 copper tubes (do = 14 mm, e = 1 mm)	37 copper tubes (do = 14 mm, e = 1 mm)
Internal configuration	Coaxial channel (do = 64 mm, di = 60 mm)	No internal channel
Distributor interiors	Tubes cross two distributors	Distributors have no tubes within
Number of distributors	4 units	2 units
Nozzle configuration	6 nozzles (di = 25 mm)	4 nozzles (di = 25 mm)
Shell dimensions	Ds = 130 mm; L = 620 mm	Ds = 130 mm, L = 620 mm
Distributor spacing	Last: 42 mm; First: 35 mm	Uniform: 42 mm
Tube sheets	Copper with metallic glue and silicone	Copper with metallic glue and silicone
Exchange surface	0.7552 m²	0.9066 m²
Insulation material	Polystyrene	Polystyrene
Flow arrangement	One pass (shell and tube sides)	One pass (shell and tube sides)

The CWST heat exchanger (Figures 7-13) derived from the STHE, was developed by removing 12 tubes from the STHE in order to insert a larger-diameter coaxial channel. The length of the 7 tubes inside the coaxial channel has been extended to pass through the first two distributors and reach the two last distributors' tube sheets. The originality of the CWST exchanger comes from the fact that it has a wide coaxial channel with tubes inside and tubes outside this channel, in

addition to having four distributors instead of the two typically found in STHEs. The comparative Table 2 exposes the information relative to the CWST heat exchanger.

3. THEORETICAL CALCULATION

The heat exchangers experimented on the test bench circulate water in counter-current and have inlet temperatures and material properties shown in Table 3. A theoretical calculation on the STHE was carried out to obtain outlet temperatures that were compared with those of the two tested heat exchangers.

Table 3. Properties of the material

Properties	Value
Density of water ρ [kg/m^3]	997
Thermal conductivity of water λ [W/(m·K)]	0.61
Dynamic viscosity of water μ [Pa·s]	0.000855
Tube thermal conductivity λ_t [W/(m·K)]	387.6
Heat capacity coefficient at constant pressure of water Cp [J/(kg·K)]	4170
Tube inlet temperature of water Tt_i [°C]	31
Shell inlet temperature of water Ts_i [°C]	18

The calculation steps that provide us with the output temperatures are as follows:

1) Calculation of the Nusselt Nu_t inside the tubes: to do this, we use the Nitsche correlation [33] for lamimar flows (Re < 2300), after calculating the Reynolds number Re_t and the Prandtl number Pr as follows:

$$Re_t = \frac{G_t \cdot di}{\mu} \tag{1}$$

$$Pr = \frac{\mu \cdot Cp}{\lambda} \tag{2}$$

$$Nu_t = 1.86 \cdot \left[\frac{Re_t \cdot Pr \cdot di}{L} \right]^{0.33} \tag{3}$$

2) Calculation of the Nusselt Nu_s inside the shell: for this purpose, we use the Prończuk-Krzanowska correlation [34], and we calculate the equivalent diameter d_{eq} for the triangular pattern, then the Reynolds number Re_s as follows:

$$d_{eq} = 4 \cdot \frac{\left(\frac{Pt^2 \cdot \sqrt{3}}{4} - \frac{\pi \cdot do^2}{8} \right)}{\frac{\pi \cdot do}{2}} \tag{4}$$

$$Re_s = \frac{G_s \cdot d_{eq}}{\mu} \tag{5}$$

$$Nu_s = 0.0813 \cdot \left[Re_s \right]^{0.834} \cdot \left[Pr \right]^{0.33} \tag{6}$$

3) Overall heat transfer coefficient K calculation: for this purpose, we calculate the convection heat transfer coefficients inside and outside the tubes (h_t and h_s) and the average exchange surface S_m as follows:

$$h_t = \frac{Nu_t \cdot \lambda}{di} \tag{7}$$

$$h_s = \frac{Nu_s \cdot \lambda}{d_{eq}} \tag{8}$$

$$S_m = \frac{\pi \cdot \left[di + (di + 2 \cdot e) \right] \cdot L \cdot Nt}{2} \tag{9}$$

$$K \cdot S_m = \frac{1}{\frac{1}{h_s \cdot \pi \cdot (di + 2 \cdot e) \cdot L \cdot Nt} + \frac{1}{h_t \cdot \pi \cdot di \cdot L \cdot Nt} + \frac{ln(\frac{di + 2 \cdot e}{di})}{2 \cdot \pi \cdot \lambda_t \cdot L \cdot Nt}} \tag{10}$$

$$K = \frac{K \cdot S_m}{S_m} \tag{11}$$

4) Calculation of the heat transfer rate ϕ: to do this, we calculate the efficiency ε, the NTU and the maximum heat transfer rate ϕ_{max} as follows [35]:

$$NTU = \frac{K \cdot S_m}{(qm \cdot Cp)_{min}} \tag{12}$$

$$Cr = \frac{(qm \cdot Cp)_{min}}{(qm \cdot Cp)_{max}} \tag{13}$$

$$\varepsilon = 2 \cdot \left[1 + Cr + (1 + Cr^2)^{\frac{1}{2}} \cdot \frac{1 + exp\left[-NTU \cdot (1 + Cr^2)^{\frac{1}{2}} \right]}{1 - exp\left[-NTU \cdot (1 + Cr^2)^{\frac{1}{2}} \right]} \right]^{-1} \tag{14}$$

$$\phi_{max} = (qm \cdot Cp)_{min} \cdot (Tt_i - Ts_i) \tag{15}$$

$$\phi = \phi_{max} \cdot \varepsilon \tag{16}$$

5) Calculation of outlet temperatures Tt_o and Ts_o: by using the heat transfer rate ϕ as follows:

$$Tt_o = Tt_i - \frac{\phi}{qm_t \cdot Cp} \tag{17}$$

$$Ts_o = \frac{\phi}{qm_s \cdot Cp} + Ts_i \tag{18}$$

4. RESULTS

4.1 Outlet temperature

Table 4 shows experimental outlet temperatures of CWST and STHE, compared with those of the STHE obtained from the theoretical calculation. These temperatures are provided by temperature sensors having an accuracy of 0.5 °C, and by

maintaining the cold fluid's flow rate while changing the hot fluid's flow rate (the cold fluid's flow rate entering through the STHE is equal to 7.7 l/min, and for the CWST exchanger, as it has two cold fluid inlets, it is equal to 3.5 l/min for the part entering through the shell and 4.2 l/min for the part entering through the last distributor).

We notice that the experimental outlet temperatures of the STHE are close to those of the theoretical calculation. The experimental output temperatures of the CWST exchanger are also close to those of the theoretical calculation, especially those for the hot fluid. However, as this CWST exchanger has two outlets for the cold fluid, there is a slight difference between the experimental temperatures of the cold fluid leaving from the shell and those from the STHE (experimental or theoretical).

4.2 Heat transfer rate

Figure 14 presents a comparative analysis of the experimental heat transfer rates for STHE and CWST as a function of the hot fluid volume flow rate. Throughout these trials, the cold fluid flow rate was maintained at a constant 7.7 l/min. Additionally, the experimental data are evaluated against the theoretical heat transfer rate predictions for the STHE.

When the volume flow rate of the hot fluid grows, the heat transfer rates in the heat exchangers also grow, which can be explained by the enhancement of convection (Note that the theoretical heat transfer rate increase of the STHE is smaller than the experimental heat transfer rates). It can also be noted that the heat transfer rates of the CWST heat exchanger are close to those of the STHE (theoretical and experimental) despite the reduction in its exchange tube surface area, and this has been demonstrated numerically in the article of Medjdoub et al. [30] for low volume flow rates.

4.3 Heat flux

Figure 15 depicts the experimental heat flux for both the STHE and CWST heat exchangers as a function of the hot fluid volume flow rate, with the cold fluid volume flow rate held constant at 7.7 l/min. These experimental values are compared against the theoretical heat flux for the STHE; both were calculated using the heat transfer rates from Figure 14 and the average tubular exchange areas specified in Table 2.

As in Figure 14, the heat fluxes of the heat exchangers rise as the volume flow rate of the hot fluid increases, and it can be observed that the heat fluxes of the CWST heat exchanger are greater than those of the STHE (theoretical and experimental), and this fact has also been shown numerically in Medjdoub et al. [30].

The observed increase in heat flux with the hot fluid flow rate is attributed to the intensification of convective transport mechanisms. Specifically, as the Reynolds number increases, the thinning of the thermal boundary layer reduces the conductive resistance at the fluid-solid interface. This leads to a steeper temperature gradient at the wall, thereby enhancing the rate of heat transfer. Furthermore, higher flow rates contribute to a more effective fluid distribution within the heat exchanger channels, ensuring that the heat transfer surface is utilized more efficiently.

Table 4. Heat exchangers outlet temperatures

	Outlet Temperature of Hot Fluid [°C]				Outlet Temperature of Shell Fluid [°C]				Outlet Temperature of Last Distributor [°C]			
Hot fluid volume flow rate [l/min]	9.5	8.5	7.5	6.5	9.5	8.5	7.5	6.5	9.5	8.5	7.5	6.5
Coaxial with shell-and-tube heat exchanger (CWST)	27.5	27.5	27	27	23	22.5	22.5	22	21.5	21	21	21
Shell-and-tube heat exchanger (STHE)	27.5	27.5	27.5	27.5	22	21.5	21	21	-	-	-	-
Theoretical calculation	27.96	27.7	27.37	26.83	21.76	21.63	21.52	21.51	-	-	-	-

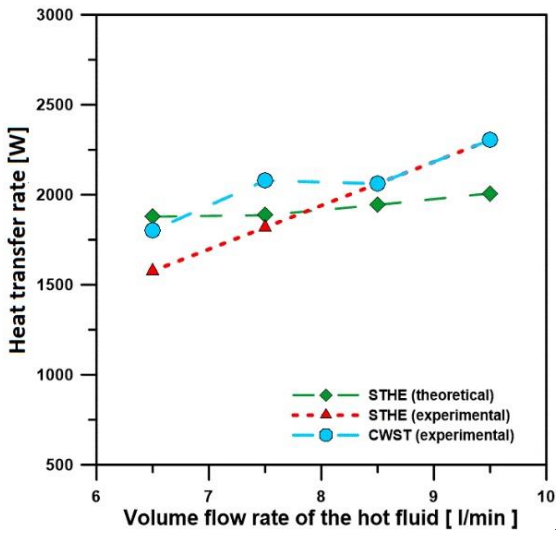

Figure 14. Heat transfer rate versus hot fluid volume flow rate curves

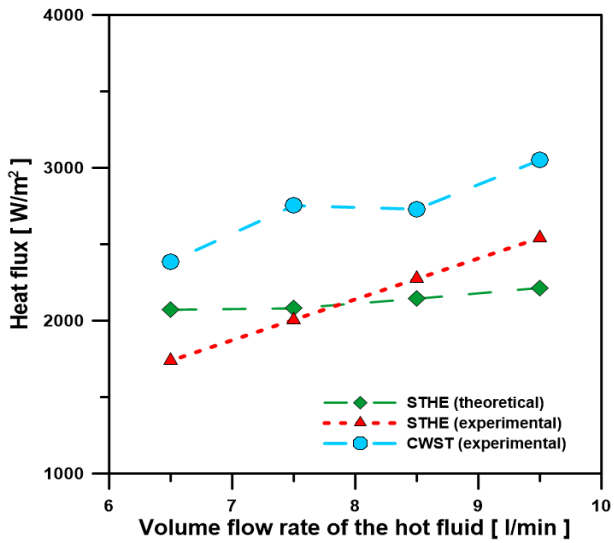

Figure 15. Curves of heat flux versus hot fluid volume flow rate

Table 5. Pressure drop and heat transfer rate to pressure drop ratio of shell-and-tube heat exchangers (STHE) and coaxial with shell-and-tube heat exchanger (CWST)

	Shell-and-Tube Heat Exchanger (STHE)	Coaxial with Shell-and-Tube Heat Exchanger (CWST)	Differences [%]
Pressure drop [psi]	3.00	1.00	-66.66
Heat transfer rate/Pressure drop [W/psi]	767.98	2303.94	+200

4.4 Heat transfer rate to pressure drop ratio and pressure drop

Table 5 shows the heat transfer rate to pressure drop ratio and pressure drop of the STHE and CWST heat exchangers, which were obtained experimentally, using pressure sensors at the heat exchangers' inlets and outlets. Due to the lack of resolution of pressure sensors having a 1psi pitch, pressure drop and the heat transfer rate to pressure drop ratio were only tested for a cold fluid volume flow rate of 7.7 l/min (for the CWST exchanger, this volume flow rate was divided into 3.5 l/min for the part passing through the shell and 4.2 l/min for the part entering via the last distributor) and a hot fluid volume flow rate of 9.5 l/min.

The heat transfer rate to pressure drop ratio is defined as the quotient between the heat transfer rate (W) and the pressure drop (psi). This metric, expressed in W/psi, is used to evaluate the balance between thermal energy gain and the mechanical energy cost.

We note that the pressure drop of the CWST exchanger is smaller than that of the STHE, and therefore it provides a greater heat transfer rate to pressure drop ratio than the STHE (this fact was also observed numerically in the article of Medjdoub et al. [32]). Although these experimental measurements are restricted to a single operating point, they provide a necessary physical baseline that aligns with the numerical trends previously reported. These results should be considered as a preliminary experimental confirmation of the CWST's hydraulic advantage, pending further investigations across a broader range of flow conditions to fully characterize the pressure drop behavior.

5. CONCLUSIONS

In this article, an experimental investigation was conducted on the CWST heat exchanger in comparison with the STHE, and a theoretical calculation on the STHE was carried out to compare its results with the experimental ones. This study led to the following conclusions:

- The CWST exchanger achieves a greater heat flux than the STHE for hot fluid volume flow rates inside the tubes varying from 6.5 l/min to 9.5 l/min and with a cold fluid volume flow rate of 7.7 l/min.
- The CWST heat exchanger delivers heat transfer rates close to those of the STHE for the low volume flow rates studied in this scientific paper.
- The CWST exchanger results in a lower pressure drop than the STHE, and therefore favors an increase of its heat transfer rate to pressure drop ratio.
- The experimental results obtained in this article are in line with the simulation results obtained in the article of Medjdoub et al. [32].
- The results obtained by theoretical calculation for the STHE are close to those obtained experimentally.

Future research will focus on broadening the operating range of the CWST heat exchanger, notably by investigating fluids with different viscosities. The development of generalized correlations based on dimensionless numbers will be essential to optimize the geometric parameters and ensure the reliability of the system when scaled up to industrial dimensions.

REFERENCES

[1] Hussain, E.S., Suhael, S.M. (2025). Optimization of HVAC systems: Advances in thermofluid performance modeling and intelligent control strategies. Power Engineering and Engineering Thermophysics, 4(1): 58-85. https://doi.org/10.56578/peet040105

[2] Lazim, A.A., Daneh-Dezfuli, A., Habeeb, L.J. (2024). Numerical analysis of heat transfer enhancement using Fe_3O_4 nanofluid under variable magnetic fields. Power Engineering and Engineering Thermophysics, 3(1): 1-11. https://doi.org/10.56578/peet030101

[3] Tan, X., Zhu, D., Zhou, G., Yang, L. (2013). 3D numerical simulation on the shell side heat transfer and pressure drop performances of twisted oval tube heat exchanger. International Journal of Heat and Mass Transfer, 65: 244-253. https://doi.org/10.1016/j.ijheatmasstransfer.2013.06.011

[4] Zhang, X.X., Wei, G.H., Sang, Z.F. (2007). Experimental research of heat transfer and flow friction properties in twisted tube heat exchanger. Huaxue Gongcheng (Chemical Engineering), 35(2): 17-20.

[5] Dizaji, H.S., Jafarmadar, S., Abbasalizadeh, M., Khorasani, S. (2015). Experiments on air bubbles injection into a vertical shell and coiled tube heat exchanger; exergy and NTU analysis. Energy Conversion and Management, 103: 973-980. https://doi.org/10.1016/j.enconman.2015.07.044

[6] Genić, S.B., Jaćimović, B.M., Jarić, M.S., Budimir, N.J., Dobrnjac, M.M. (2012). Research on the shell-side thermal performances of heat exchangers with helical tube coils. International Journal of Heat and Mass Transfer, 55(15-16): 4295-4300. https://doi.org/10.1016/j.ijheatmasstransfer.2012.03.074

[7] Zhang, J., Guo, S., Li, Z., Wang, J., He, Y., Tao, W. (2013). Experimental performance comparison of shell-and-tube oil coolers with overlapped helical baffles and segmental baffles. Applied Thermal Engineering, 58(1-2): 336-343. https://doi.org/10.1016/j.applthermaleng.2013.04.009

[8] Xiao, X., Zhang, L., Li, X., Jiang, B., Yang, X., Xia, Y. (2013). Numerical investigation of helical baffles heat exchanger with different Prandtl number fluids. International Journal of Heat and Mass Transfer, 63: 434-444. https://doi.org/10.1016/j.ijheatmasstransfer.2013.04.001

[9] Li, N., Chen, J., Cheng, T., Klemeš, J.J., Varbanov, P.S., Wang, Q., Zeng, M. (2020). Analysing thermal-hydraulic performance and energy efficiency of shell-and-tube heat exchangers with longitudinal flow based on experiment

and numerical simulation. Energy, 202: 117757. https://doi.org/10.1016/j.energy.2020.117757
[10] Ben Slimene, M., Poncet, S., Bessrour, J., Kallel, F. (2022). Numerical investigation of the flow dynamics and heat transfer in a rectangular shell-and-tube heat exchanger. Case Studies in Thermal Engineering, 32: 101873. https://doi.org/10.1016/j.csite.2022.101873
[11] Ali, M.R., Al-Khaled, K., Hussain, M., Labidi, T., Khan, S.U., Kolsi, L., Sadat, R. (2022). Effect of design parameters on passive control of heat transfer enhancement phenomenon in heat exchangers–A brief review. Case Studies in Thermal Engineering, 43: 102674. https://doi.org/10.1016/j.csite.2022.102674
[12] Yang, J., Liu, W. (2015). Numerical investigation on a novel shell-and-tube heat exchanger with plate baffles and experimental validation. Energy Conversion and Management, 101: 689-696. https://doi.org/10.1016/j.enconman.2015.05.066
[13] Chen, J., Li, N., Ding, Y., Klemeš, J.J., Varbanov, P.S., Wang, Q., Zeng, M. (2020). Experimental thermal-hydraulic performances of heat exchangers with different baffle patterns. Energy, 205: 118066. https://doi.org/10.1016/j.energy.2020.118066
[14] Wang, X., Liang, Y., Sun, Y., Liu, Z., Liu, W. (2019). Experimental and numerical investigation on shell-side performance of a double shell-pass rod baffle heat exchanger. International Journal of Heat and Mass Transfer, 132: 631-642. https://doi.org/10.1016/j.ijheatmasstransfer.2018.12.046
[15] Liu, J., Liu, Z., Liu, W. (2015). 3D numerical study on shell side heat transfer and flow characteristics of rod-baffle heat exchangers with spirally corrugated tubes. International Journal of Thermal Sciences, 89: 34-42. https://doi.org/10.1016/j.ijthermalsci.2014.10.011
[16] Ji, J., Ge, P., Bi, W. (2016). Numerical analysis on shell-side flow-induced vibration and heat transfer characteristics of elastic tube bundle in heat exchanger. Applied Thermal Engineering, 107: 544-551. https://doi.org/10.1016/j.applthermaleng.2016.07.018
[17] Bougriou, C., Baadache, K. (2010). Shell-and-double concentric-tube heat exchangers. Heat and Mass Transfer, 46(3): 315-322. https://doi.org/10.1007/s00231-010-0572-z
[18] Van Trang, N., Trung, D.T., Van Dzung, D. (2017). Experimental study of alternative minichannel heat exchanger for scooter radiator. International Journal of Emerging Research in Management and Technology, 6(4): 46-50. https://doi.org/10.23956/ijermt/v6n4/116
[19] Lozano, A., Barreras, F., Fueyo, N., Santodomingo, S. (2008). The flow in an oil/water plate heat exchanger for the automotive industry. Applied Thermal Engineering, 28(10): 1109-1117. https://doi.org/10.1016/j.applthermaleng.2007.08.015
[20] Elias, M., Shahrul, I., Mahbubul, I., Saidur, R., Rahim, N. (2014). Effect of different nanoparticle shapes on shell and tube heat exchanger using different baffle angles and operated with nanofluid. International Journal of Heat and Mass Transfer, 70: 289-297. https://doi.org/10.1016/j.ijheatmasstransfer.2013.11.018
[21] Leong, K., Saidur, R., Mahlia, T., Yau, Y. (2012). Modeling of shell and tube heat recovery exchanger operated with nanofluid based coolants. International Journal of Heat and Mass Transfer, 55(4): 808-816. https://doi.org/10.1016/j.ijheatmasstransfer.2011.10.027
[22] Elias, M., Miqdad, M., Mahbubul, I., Saidur, R., Kamalisarvestani, M., Sohel, M., Hepbasli, A., Rahim, N., Amalina, M. (2013). Effect of nanoparticle shape on the heat transfer and thermodynamic performance of a shell and tube heat exchanger. International Communications in Heat and Mass Transfer, 44: 93-99. https://doi.org/10.1016/j.icheatmasstransfer.2013.03.014
[23] Philip, J., Shima, P.D., Raj, B. (2008). Nanofluid with tunable thermal properties. Applied Physics Letters, 92: 043108. https://doi.org/10.1063/1.2838304
[24] Yu, W., Xie, H., Wang, X., Wang, X. (2011). Significant thermal conductivity enhancement for nanofluids containing graphene nanosheets. Physics Letters A, 375(10): 1323-1328. https://doi.org/10.1016/j.physleta.2011.01.040
[25] Touatit, A., Bougriou, C. (2018). Optimal diameters of triple concentric-tube heat exchangers. International Journal of Heat and Technology, 36(1): 367-375. https://doi.org/10.18280/ijht.360149
[26] Xie, G., Wang, Q., Zeng, M., Luo, L. (2007). Heat transfer analysis for shell-and-tube heat exchangers with experimental data by artificial neural networks approach. Applied Thermal Engineering, 27(5-6): 1096-1104. https://doi.org/10.1016/j.applthermaleng.2006.07.036
[27] Fettaka, S., Thibault, J., Gupta, Y. (2013). Design of shell-and-tube heat exchangers using multiobjective optimization. International Journal of Heat and Mass Transfer, 60: 343-354. https://doi.org/10.1016/j.ijheatmasstransfer.2012.12.047
[28] Guo, J., Cheng, L., Xu, M. (2009). Optimization design of shell-and-tube heat exchanger by entropy generation minimization and genetic algorithm. Applied Thermal Engineering, 29(14-15): 2954-2960. https://doi.org/10.1016/j.applthermaleng.2009.03.011
[29] Şahin, A.Ş., Kılıç, B., Kılıç, U. (2011). Design and economic optimization of shell and tube heat exchangers using Artificial Bee Colony (ABC) algorithm. Energy Conversion and Management, 52(11): 3356-3362. https://doi.org/10.1016/j.enconman.2011.07.003
[30] Guo, J., Xu, M., Cheng, L. (2009). The application of field synergy number in shell-and-tube heat exchanger optimization design. Applied Energy, 86(10): 2079-2087. https://doi.org/10.1016/j.apenergy.2009.01.013
[31] Fesanghary, M., Damangir, E., Soleimani, I. (2009). Design optimization of shell and tube heat exchangers using global sensitivity analysis and harmony search algorithm. Applied Thermal Engineering, 29(5-6): 1026-1031. https://doi.org/10.1016/j.applthermaleng.2008.05.018
[32] Medjdoub, C., Benslimane, A., Sadaoui, D., Bekkour, K. (2024). Numerical investigation of mass and heat transfer in a new coaxial with shell-and-tube heat exchanger. Mathematical Modelling of Engineering Problems, 11(7): 110701. https://doi.org/10.18280/mmep.110701
[33] Nitsche, M., Gbadamosi, R. (2016). Heat Exchanger Design Guide. Elsevier. https://doi.org/10.1016/c2014-0-04971-4
[34] Prończuk, M., Krzanowska, A. (2021). Experimental investigation of the heat transfer and pressure drop inside tubes and the shell of a minichannel shell and tube type heat exchanger. Energies, 14(24): 8563. https://doi.org/10.3390/en14248563
[35] Incropera, F.P., Dewitt, D.P., Bergman, T.L., Lavine,

A.S. (2007). Fundamentals of Heat and Mass Transfer. John Wiley & Sons.

NOMENCLATURE

Cp	heat capacity coefficient at constant pressure, J/(kg·K)
d	diameter, m
di	inside diameter of a tube, m
do	outside diameter of a tube, m
Ds	inside diameter of the shell, m
e	thickness of a tube, m
G	surface flow rate, kg/(m^2·s)
h	convection coefficient, W/(m^2·K)
K	overall heat transfer coefficient, W/(m^2·K)
L	length of the shell, m
Nt	number of tubes
Nu	Nusselt number
Pr	Prandtl number
PR	ratio of the pitch to the outside diameter of a tube
Pt	pitch, m
qm	mass flow rate, kg/s
Re	Reynolds number
S	section, m^2
Tt	temperature of tube side (hot fluid), K
Ts	temperature of the shell side (cold fluid), K

Greek symbols

ε	efficiency
λ	thermal conductivity, W/m·K
μ	dynamic viscosity, Pa·s
ρ	density, kg/m^3
ϕ	heat transfer rate, W

Subscripts

i	input
eq	equivalent
m	average
max	maximum
min	minimum
o	output
s	shell side
t	tube side

Abbreviation

CWST	the coaxial with shell-and-tube heat exchanger
STHE	shell-and-tube heat exchanger
NTU	number of transfer units